Broadband Measurements of Nanofiber Devices: Repeatability and Random Error Analysis*

T. Mitch Wallis[1], Atif Imtiaz[1], Sang-Hyun Lim[1], and Pavel Kabos[1]
[1]Electromagnetics Division
National Institute of Standards and Technology
Boulder, Colorado, USA
Correspondence: mwallis@boulder.nist.gov

Kichul Kim[2], Paul Rice[3], and Dejan Filipovic[2]
[2]Department of Electrical, Computer, and Energy Engineering
[3]Nanomaterials Characterization Facility
University of Colorado
Boulder, Colorado, USA

***Abstract*—On-wafer, broadband measurements of two-port nanofiber devices were made in order to test the short-term repeatability of a widely used measurement approach that builds on established on-wafer calibration techniques. The test devices used in this study consist of Pt nanowire and Au microbridge structures incorporated into two-port coplanar waveguides. Based on repeated measurements of these test structures, we computed statistical (Type A) uncertainties. The standard deviation (k=1) of five repeated measurements of a Pt nanowire device was less than 50 μS. The analysis suggests refinements to the measurement process depending on the desired output of the measurements, e.g. the broadband response itself or the extraction of circuit model parameters.**

Index Terms- Microwave measurements, Nanotechnology, Nanowires, On-wafer devices, Calibration

I. INTRODUCTION

There is ongoing interest in nanofiber materials such as carbon nanotubes and nanowires as their unique material and electrical properties present the possibility for new applications. For example, carbon nanotube-based transistors are expected to have extremely high cutoff frequencies, perhaps in the terahertz regime [1]. Semiconducting nanowires are being integrated into new optoelectronic applications such as nanowire-based light emitting diodes. Historically, electrical characterization of nanofiber materials focused on DC methods. However, as broadband applications of nanofiber-based devices have been developed, corresponding on-wafer, broadband metrology has emerged. Originally, many of these measurement methods were applied to individual carbon nanotubes and on-wafer, carbon nanotube-based devices [1-5]. More recently, these methods have been extended to devices that incorporate semiconducting and metallic nanowires [6-8].

In general, broadband characterization of nanofiber devices faces several challenges, including significant impedance mismatch between the nanofiber devices and commercial 50 Ω test equipment. Often, transmission through the device is dominated by stray capacitive coupling. Additionally, the broadband response of such a device may be dominated by the response of the contacts to the nanofiber. A number of approaches have been developed to overcome these problems. For instance, a matching network may be used to compensate for the impedance mismatch. However, matching networks may limit the measurement bandwidth and if one wishes to extract properties of the nanofiber, the matching network will subsequently have to be de-embedded from the measurement. Alternatively, an array of parallel nanofibers may be used to produce a device that is impedance matched to 50 Ω. While this approach is particularly promising for applications such as field effect transistors, it relies upon the production of a large number of identical, semiconducting nanofibers which is still a significant challenge [9, 10]. Randus and Hoffman have pioneered an approach to extreme impedance measurements based on hybrid couplers [11-13]. Conceivably, this method might be extended to on-wafer devices, but so far it has only been demonstrated in coaxial systems.

In this paper, we will focus on one of the most widely used approaches for on-wafer, broadband characterization of nanofiber-based devices [1-8]. This approach relies upon two key elements: (i) the use of established on-wafer calibration techniques to de-embed the measured device response and (ii) the measurement of empty, nanofiber-free devices in order to account for stray capacitance. Though any suitable on-wafer calibration technique may be used in this approach, we will focus on the multiline Thru-Reflect-Line (TRL) calibration [14]. TRL is a well-known, reliable approach to on-wafer calibration and as the propagation constant is a by-product of the TRL calibration, the reference planes can be moved as close as possible to the point where the contacts are made to the nanofiber within the device. The validity of this measurement framework for characterization of nanofiber devices has been tested through numerous measurements as well as comparison to finite-element and circuit-based simulations [8]. However, there has been no systematic study of the uncertainties associated with this measurement process. In fact, there is very little documentation of either the long-term or the short-term repeatability of this measurement process. In this paper, we present measurements of the repeatability of this measurement process and an analysis of the statistical (Type A) uncertainties associated with it. The analysis suggests certain refinements to the measurement process depending on the objective of the measurements, e.g. the broadband response itself or the extraction of model circuit parameters.

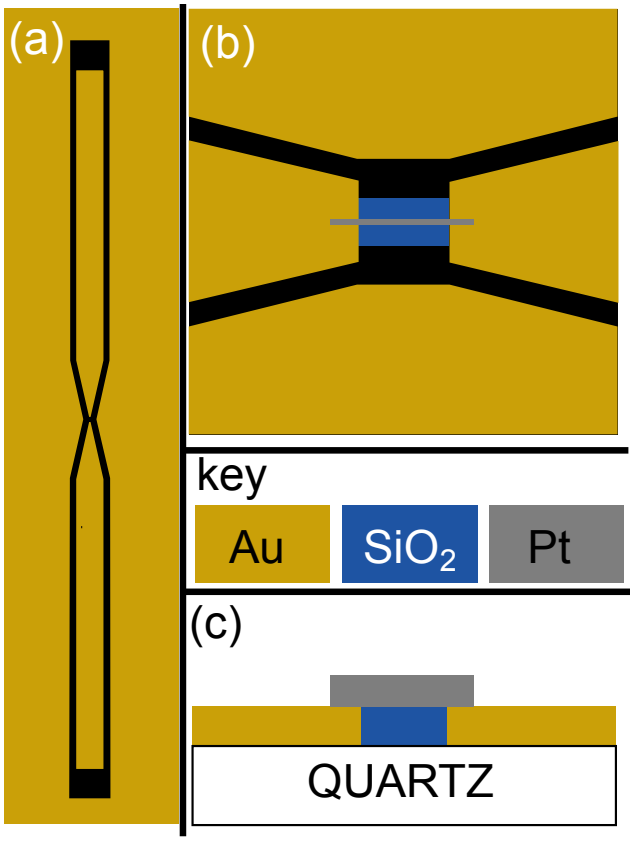

Figure 1. (a) Schematic of the two-port, CPW test devices. (b) Magnified schematic (top view) of the CPW gap region where an SiO_2-supported Pt nanowire bridges the gap. (c) Magnified schematic (side view) of the CPW gap region. In side view, dimensions are not to scale.

II. Test Devices

Two-port, on-wafer test devices were fabricated to perform the repeatability and uncertainty analysis for broadband measurements of nanofiber-based devices, as shown in Figure 1. The test device design for the broadband characterization of a variety of systems, including GaN [7] and Pt [8] nanowires has been introduced elsewhere. The test devices consist of a 1200 µm-long coplanar waveguide (CPW) divided into two segments by a 16 µm gap in the center conductor. These CPW test devices serve as a host for nanofibers that may be fabricated or deposited in such a way so that they bridge the gap between the two CPW segments. The 100 µm of CPW center conductor to either side of the gap in each device are tapered to constrain the region where nanofibers may bridge the gap. The CPW ground contacts are tapered along with the center conductor so as to maintain a constant distance between center conductor and ground plane. The test devices were fabricated by use of standard photolithographic techniques on quartz substrates and consist of a 200 nm Au layer deposited on top of a 20 nm Ti adhesion layer. Pt nanowires were deposited in the gaps of selected test devices by use of a focused ion beam system. Initially, a SiO_2 support layer was deposited between the electrodes. Then, Pt nanowires (about 250 nm in diameter) were deposited across the gap, with about 3 µm of Pt overlapping the center conductor electrode to form contacts. In addition to the devices with Pt nanowires, devices with lithographically-defined, 2 µm-wide Au lines were fabricated. Finally, a set of on-wafer calibration standards, including a thru, a short and transmission lines of various lengths, were fabricated on the same wafer in order to perform the TRL calibration. Note that the CPW geometry in the non-tapered segments of the test devices was designed to have an impedance of 50 Ω. The DC resistance of the Pt nanowire devices was on the order of a few kilohms.

Nanowire devices, Au microbridge devices, empty (nanowire-free) devices, and calibration standards were contacted with commercial ground-signal-ground (GSG) probes. Measurements were made with a commercial vector network analyzer. The TRL calibration and the movement of the reference planes were performed by use of the NISTCal software package [15]. It was particularly important to avoid static discharge through the Pt nanowire devices as modest static discharge currents may alter or even burn out the Pt nanowire contacts. To prevent static discharge currents, the GSG probes were shorted between repeated measurements of the devices by contacting the probes to continuous metal films. Between the repeated measurements of the same device: (i) both probes were lifted from the device under test, (ii) both probes were moved and contacted to a continuous metal film, thus shorting them to one another, (iii) both probes were lifted an moved back to the device under test, and (iv) both probes were re-contacted to the device under test.

III. Measurement Process

The measurement process for broadband characterization of nanofiber devices builds upon established on-wafer calibration techniques. Calibrated on-wafer measurements provide the two input quantities for this process. The first input quantity is the calibrated scattering parameter matrix of an "empty", nanofiber-free device with the reference planes moved to the start of the tapered section of the CPW center conductor. The elements of this first input matrix, S^{gap}_{ij} (i = 1,2; j = 1,2). The second input quantity is the calibrated scattering parameter matrix of a nanofiber device also with the reference planes moved to the start of the tapered section of the CPW center conductor. The elements of this second input matrix are S^{dev}_{ij} (i = 1,2; j = 1,2). The objective is to find the calibrated scattering parameter matrix of the contacted nanofiber, S^{nf}_{ij} (i = 1,2; j = 1,2). In the measurement model, the stray capacitance is assumed to be in parallel with the contacted nanowire. If the scattering parameter matrices, $\boldsymbol{S}^{gap}$, $\boldsymbol{S}^{dev}$ and $\boldsymbol{S}^{nf}$ are converted to an admittance matrix representation, $\boldsymbol{Y}^{gap}$, $\boldsymbol{Y}^{dev}$ and $\boldsymbol{Y}^{nf}$, the underlying assumption of the model can be expressed in a simple algebraic form:

$$Y^{nf} = Y^{dev} - Y^{gap} \quad . \qquad (1)$$

Since $\boldsymbol{Y}^{gap}$ and $\boldsymbol{Y}^{dev}$ are known from the measurements, $\boldsymbol{Y}^{nf}$ may be calculated from equation (1). In some instances, $\boldsymbol{Y}^{nf}$

may be the only desired output of the measurement process. However, it is often also desirable to extract additional information about the nanofiber, such as the series resistance of the contacts and the series resistance of the nanofiber. In order to extracts such quantitites, $\boldsymbol{Y}^{nf}$ must be compared to an appropriate circuit model. The establishment of broadly applicable, accurate circuit models for such systems is an ongoing area of research. The extraction of model circuit parameters from broadband measurements of nanofiber devices is discussed in further detail in Section V below.

IV. Repeatability and Random Error Analysis

A. Uncertainty Analysis

As described above, the measurement process has two inputs, namely the scattering matrix elements $S^{gap}{}_{ij}$ and $S^{dev}{}_{ij}$, which are obtained from calibrated on-wafer measurements. We will refer to the uncertainties in these matrix elements as $\Delta S^{gap}{}_{ij}$ and $\Delta S^{dev}{}_{ij}$ and we will assume that these uncertainties are known from the calibrated on-wafer measurement process. As the scattering matrix elements are transformed into an admittance matrix representation, the uncertainties propagate in the usual way:

$$\Delta Y_{ij}^{gap} = \sqrt{\frac{\left(\Delta Y_{ij}^{Agap}\right)^2}{N_{emptydev}} + \sum_{k,l}\left(\frac{\partial Y_{ij}^{gap}}{\partial S_{kl}^{gap}}\Delta S_{kl}^{gap}\right)^2} \qquad (2)$$

and

$$\Delta Y_{ij}^{dev} = \sqrt{\sum_{k,l}\left(\frac{\partial Y_{ij}^{dev}}{\partial S_{kl}^{dev}}\Delta S_{kl}^{dev}\right)^2} \quad . \qquad (3)$$

Multiple empty devices were measured in order to account for variations in fabrication and substrate properties. The use of multiple empty devices leads to the inclusion of the Type A uncertainty term $\Delta Y^{Agap}{}_{ij}$ in equation (2). $N_{emptydev}$ is the number of different empty devices that were measured. In the measurements discussed below, $N_{emptydev}$ equalled five. When $Y^{gap}{}_{ij}$ and $Y^{dev}{}_{ij}$ are combined via equation (1) to produce $Y^{nf}{}_{ij}$, the resulting uncertainty is given by:

$$\Delta Y_{ij}^{nf} = \sqrt{\left(\Delta Y_{ij}^{gap}\right)^2 + \left(\Delta Y_{ij}^{dev}\right)^2 + \left(\Delta Y_{ij}^{B}\right)^2 + \frac{\left(\Delta Y_{ij}^{Anf}\right)^2}{N_{repeat}}} \quad . (4)$$

In order to test repeatability and analyze sources of random error, each nanofiber device and each "empty" device is measured multiple times, leading to the inclusion of the Type A uncertainty term $\Delta Y^{Anf}{}_{ij}$ in equation (4). N_{repeat} is the number of repeated measurements of each device. In the measurements discussed below, N_{repeat} was five. $\Delta Y^{B}{}_{ij}$ is the Type B uncertainty term and includes all systematic sources of uncertainty in the measurement model, including the validity (or lack of validity) of equation (1). The following section presents the experimental determination of the Type A uncertainty terms $\Delta Y^{Agap}{}_{ij}$, $\Delta Y^{Anf}{}_{ij}$ for a Pt nanowire device, and $\Delta Y^{Anf}{}_{ij}$ for a Au microbridge device.

B. Type A Uncertainty Terms

The mean and standard deviation of repeated measurements of $Y^{gap}{}_{ij}$ for multiple empty devices are shown in Figure 2. The admittance matrix elements are consistent with a series capacitance: $|Y^{gap}{}_{12}|$ and $|Y^{gap}{}_{21}|$ are small (on the order of tens of microSiemens) and approximately linear with frequency. In general, the standard deviation (k = 1) of multiple empty devices is only a few microsiemens through most of the measured frequency range. Nonetheless, measurements of multiple devices are highly desirable, particularly in the range above 30 GHz where there is increased noise in the data.

The mean and standard deviation of repeated measurements of $Y^{nf}{}_{ij}$ for a Pt nanowire device are shown in Figure 3. The Pt nanowire device measurements show good short-term repeatability. Note that $\Delta Y^{nf}{}_{11}$ is slightly higher than

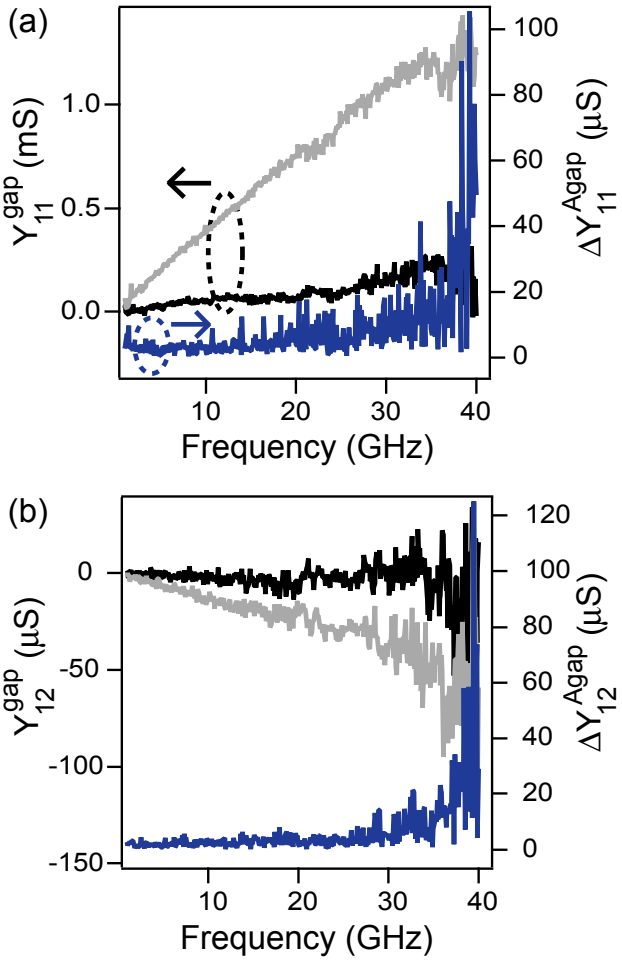

Figure 2. Calibrated admittance matrix elements of an empty (nanofiber-free) device from 1 GHz to 40 GHz. Black curves show the mean real part and gray curves show the mean imaginary part of (a) $Y^{gap}{}_{11}$ and (b) $Y^{gap}{}_{12}$. Blue curves show the standard deviation (k = 1) of the real part of measurements of five different empty devices.

ΔY^{nf}_{12} throughout the measured frequency range. The short-term repeatability measurements were made within a few minutes. However, attempts to measure the long-term repeatability of the Pt nanowire devices over several months showed a systematic drift in the measurements, most likely due to degradation of the Pt nanowires.

The mean and standard deviation of repeated measurements of Y^{nf}_{ij} for a Au microbridge device are shown in Figure 4. The Au microbridge displays extremely high transmission and little reflection through the device. Note that the magnitudes of all four elements – $|Y^{nf}_{11}|$, $|Y^{nf}_{12}|$, $|Y^{nf}_{21}|$, and $|Y^{nf}_{22}|$ – are nearly equivalent. This arises from the conversion of the scattering parameters to admittance parameters, given that S^{nf}_{21} and S^{nf}_{12} are approximately one while S^{nf}_{11} and S^{nf}_{22} are nearly zero. The Au microbridge measurements show excellent short-term repeatability. Note that each set of repeated measurements described here were made with the same on-wafer calibration.

C. *Other Uncertainty Terms*

In addition to the Type A uncertainty terms, there are two additional sources of uncertainty in equations (2), (3), and (4): the uncertainty arising from the calibrated scattering parameter measurements (ΔS^{gap}_{ij} and ΔS^{dev}_{ij}) and the Type B uncertainty in the admittance matrix of the nanofiber (ΔY^{B}_{ij}). While Type A uncertainties are generally straightforward to calculate, they tend to be of limited interest as it is well known that repeated measurements will decrease statistically-derived uncertainty. While ΔS^{gap}_{ij}, ΔS^{dev}_{ij}, and ΔY^{B}_{ij} may be of greater interest, they are also more challenging to calculate. Calculation and estimation of these uncertainty terms have been addressed elsewhere. Below, we briefly summarize the conclusions of those investigations.

All calibrated measurements described here use the TRL calibration technique. Thus, ΔS^{gap}_{ij} and ΔS^{dev}_{ij} must be determined from uncertainty analysis of the TRL measurement process. Such analysis has been undertaken by other researchers, most notably Williams, Arz, and coworkers [16-18]. Based on their work, we estimate ΔS^{gap}_{ij} and ΔS^{dev}_{ij} to be 0.005. When propagated through the transformation to the admittance matrix representation, this corresponds to an uncertainty of about 0.05 mS for high-impedance systems such as a Pt nanowire. This represents a significant fraction of

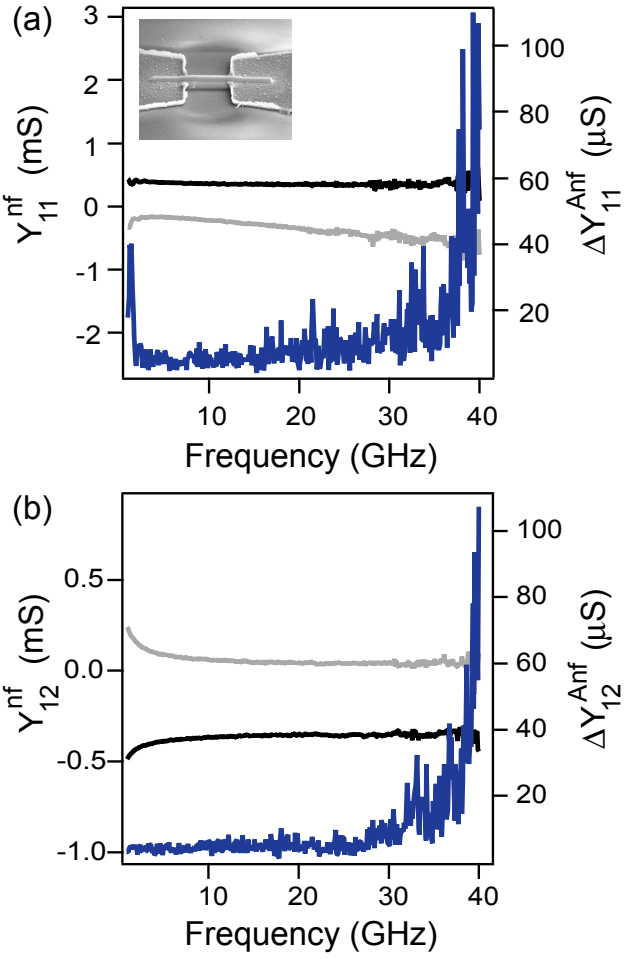

Figure 3. Calibrated admittance matrix elements of a Pt nanowire device from 1 GHz to 40 GHz. Black curves show the mean real part and gray curves show the mean imaginary part of (a) Y^{nf}_{11} and (b) Y^{nf}_{12}. Blue curves show the standard deviation (k = 1) of the real part of five repeated measurements. The inset in (a) shows a scanning electron microscope image of the Pt nanowire device.

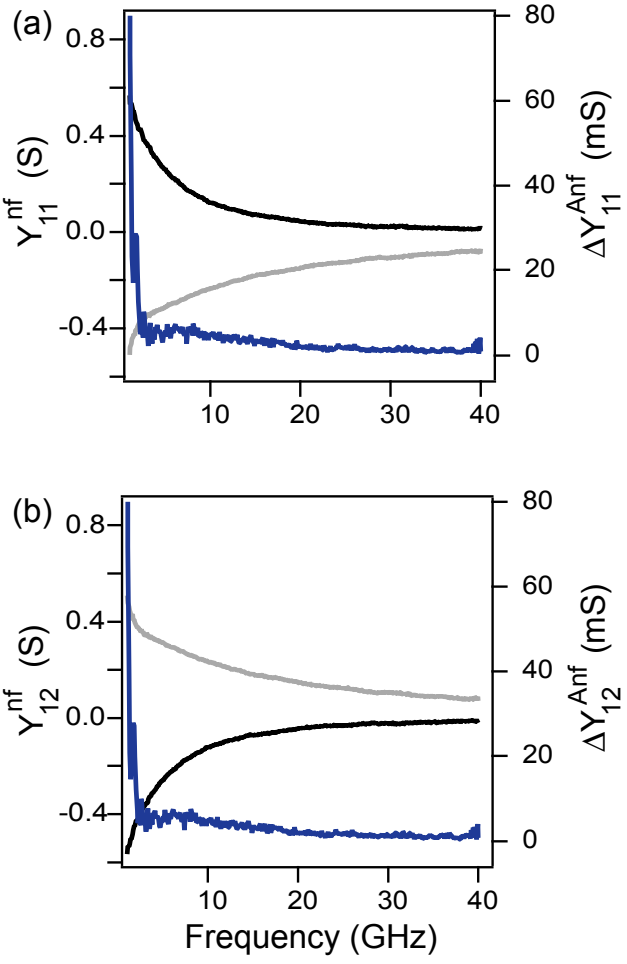

Figure 4. Calibrated admittance matrix elements of a Au microbridge device from 1 GHz to 40 GHz. Black curves show the mean real part and gray curves show the mean imaginary part of (a) Y^{nf}_{11} and (b) Y^{nf}_{12}. Blue curves show the standard deviation (k = 1) of the real part of five repeated measurements.

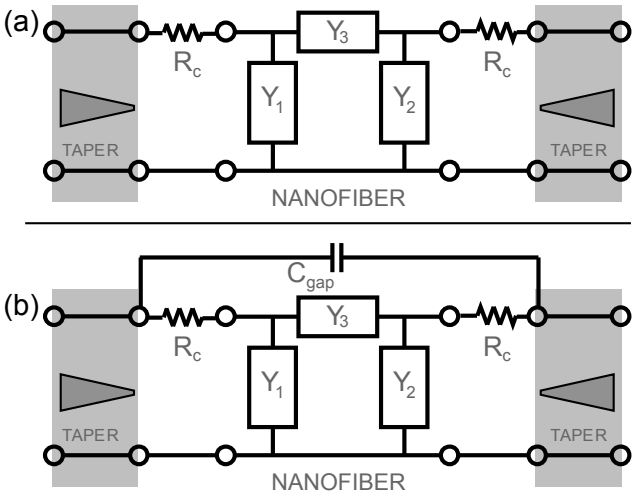

Figure 5. Cicuit models for nanofiber devices include a π-model representation of the nanofiber (Y_1, Y_2, and Y_3), contact resistance (R_c) as well as a model of the tapered section of the CPW center conductor. Circuits are shown with (a) and without (b) the stray capacitance (C_{gap}).

the measured Y^{nf}_{12} for the Pt nanowire device and a significant contribution to the overall uncertainty budget.

The uncertainty term ΔY^{B}_{ij} reflects systematic errors in the measurement framework, including systematic errors in the underlying assumptions expressed in equation (1). A systematic study of the measurement framework, including the comparison of calibrated broadband measurements of nanowire devices to finite element modeling, has been published elsewhere [8]. Based on that study, we estimate ΔY^{B}_{ij} to be 0.05 mS for a Pt nanowire device, also a significant contribution to the overall uncertainty budget.

V. Extraction of Circuit Model Parameters

In some cases, broadband measurement of $\boldsymbol{Y}^{nf}$ may represent a desirable, sufficient outcome of the measurement process. Additionally, $\boldsymbol{Y}^{nf}$ may be transformed to other representations such as scattering parameter or impedance matrices, albeit with the appropriate propagation of the uncertainties. Often, it is desirable to establish a circuit model for the nanofiber device and extract circuit parameters that may be correlated with physical properties of the device. For example, the kinetic inductance of a single carbon nanotube [4] and the junction capacitance of a Schottky contact to a GaN nanowire [8] have been extracted from broadband measurements. A schematic of a circuit model for nanofiber test devices used in this study is shown in Figure 5(a). In general, circuit models of nanofiber devices are hybrids of transmission line and lumped elements. For instance, the circuit model includes transmission line elements such as the model of the tapered part of the CPW center conductor and π-model (Y_1, Y_2, and Y_3) of the nanofiber itself, but also includes lumped elements in the form of contact resistances (R_c).

The circuit model may be compared directly to $\boldsymbol{Y}^{nf}$ in order to extract elements such as R_c, Y_1, Y_2, and Y_3. However, as shown above, there are sizable uncertainties in $\boldsymbol{Y}^{nf}$ largely due to systematic (Type B) uncertainties. An alternative approach is to fit the calibrated scattering parameter measurements, $\boldsymbol{S}^{gap}$ and $\boldsymbol{S}^{dev}$. For this alternative approach, the stray (gap) capacitance (C_{gap}) is included explicitly in the circuit model as shown in Figure 5(b). The first step is to determine C_{gap} by fitting $\boldsymbol{S}^{gap}$. The resulting value of C_{gap} may then be held fixed while $\boldsymbol{S}^{dev}$ is fitted with the model shown in Figure 5(b). For this alternate approach, the uncertainty analysis is altered in the following way:

$$\Delta S_{ij}^{gap\_tot} = \sqrt{\frac{\left(\Delta S_{ij}^{Aemptydev}\right)^2}{N_{emptydev}} + \frac{\left(\Delta S_{ij}^{Agap}\right)^2}{N_{repeat}} + \left(\Delta S_{ij}^{gap}\right)^2} \quad (5)$$

and

$$\Delta S_{ij}^{dev\_tot} = \sqrt{\frac{\left(\Delta S_{ij}^{Adev}\right)^2}{N_{repeat}} + \left(\Delta S_{ij}^{dev}\right)^2} \quad . \quad (6)$$

$\Delta S^{gap\_tot}_{ij}$ and $\Delta S^{gap\_tot}_{ij}$ are the total uncertainties in S^{gap}_{ij} and S^{dev}_{ij}, respectively, which have incorporated the Type A uncertainties from the multiple empty device measurements, $\Delta S^{Aemptydev}_{ij}$ as well as from the repeated measurements ΔS^{Agap}_{ij} and ΔS^{Adev}_{ij}. The uncertainties in the extracted circuit parameters, such as C_{gap} and R_c, may then be determined from the fitting procedure.

VI. Conclusion

The short-term repeatability and Type A uncertainties of on-wafer, broadband measurements of two-port nanofiber devices were studied. Although the measurements are highly repeatable and the Type A uncertainties are small, the total uncertainties in the admittance matrix for the nanofiber device, $\boldsymbol{Y}^{nf}$, are considerable due to contributions from systematic errors. An approach to extracting circuit parameters by fitting the calibrated scattering parameters of one empty device and one nanofiber device was introduced. Going forward, in order to place this measurement process on a more sound footing, it is necessary to establish comparisons with other broadband characterization techniques for extreme impedance devices.

References

[1] C. Rutherglen and P. J. Burke, "Nanoelectromagnetics: circuit and electromagnetic properties of carbon nanotubes," Small, vol. 5, pp. 884–906, 2009.

[2] J. M. Bethoux, H. Happy, G. Dambrine, V. Derycke, M. Goffman, and J. P. Burgoin, "An 8-GHz ft carbon nanotube field-effect transistor for gigahertz range applications," IEEE Electron Device Letters, vol. 27, pp. 681–683, 2006.

[3] M. Zhang, X. Huo, P. C. H. Chan, Q. Liang, and Z. K. Tang, "Radio-frequency characterization for the single-walled carbon nanotubes," Appl. Phys. Lett., vol. 88, art. no. 163109, 2006.

[4] J. J. Plombon, K. P. O'Brien, F. Gstrein, V. M. Dubin, and Y. Jiao, "High-frequency electrical properties of individual and bundled carbon nanotubes," Appl. Phys. Lett., vol 90, art. no. 063106, 2007.

[5] L. Nougaret, G. Dambrine, S. Lepillet, H. Hapy, N. Chimot, V. Derycke, and J. P. Burgoin, "Gigahertz characterization of a single carbon nanotube," Appl. Phys. Lett., vol. 96, art. no. 042109.

[6] S. Vandenbrouck, K. Madjour, D. Theon, Y. Dong, Y. Li, C. M. Lieber, and C. Gaquiere, "12 GHz FMAX GaN/AlN/AlGaN nanowire MISFET," IEEE Electron Device Letters, vol. 30, pp. 322-324, 2009.

[7] C. J. Chiang, T. M. Wallis, D. Gu, A. Imtiaz, P. Kabos, P. T. Blanchard, K. A. Bertness, N. A. Sanford, K. Kim, and D. Filipovic, "High frequency characterization of a Schottky contact to a GaN nanowire bundle" J. of Appl. Phys., vol. 107, art. no. 124301, 2010.

[8] K. Kim, T. M. Wallis, P. Rice, C. J. Chiang, A. Imtiaz, P. Kabos, and D. S. Filipovic, "A framework for broadband characterization of individual nanowires," IEEE Microwave and Wireless Component Lett., vol. 20, pp. 178-180, 2010.

[9] C. Rutherglen, D. Jain, and P. Burke, "RF resistance and inductance of massively parallel single walled nanotubes: direct, broadband measurements of near perfect 50 ohm impedance matching," Appl. Phys. Lett., vol. 93, art. no. 083119, 2008.

[10] S. W. Hong, T. Banks, and J. A. Rogers, "Improved density in aligned arrays of single-walled carbon nanotubes by sequential chemical vapor deposition on quartz," Advanced Materials, vol. 22, pp. 1826-1830, 2010.

[11] M. Randus and K. Hoffman, "A simpel method for extreme impedances measurement," 70th ARFTG Microwave Measurement Symposium Digest, 2007.

[12] M. Randus and K. Hoffman, "A method for extreme impedances measurement – experimental testing," 72nd ARFTG Microwave Measurement Symposium Digest, 2008.

[13] A. Lewandowski, D. LeGolvan, R. A. Ginley, T. M. Wallis, A. Imtiaz, and P. Kabos, "Wideband measurement of extreme impedances with a multistate reflectometer," 72nd ARFTG Microwave Measurement Symposium Digest, 2008.

[14] R. Marks, "A multiline method of network analyzer calibration," IEEE Trans. on Microwave Theory and Techniques, vol. 39, pp. 1205-1215, 1991.

[15] http://www.nist.gov/eeel/electromagnetics/related-software.cfm

[16] D. F. Williams, C. M. Wang, and U. Arz, "An optimal multiline TRL calibration algorithm," 2003 International Microwave Symposium Digest.

[17] J. Leinhos and U. Arz, "Monte-Carlo analysis of measurement uncertainties for on-wafer thru-reflect-line calibrations," 71st ARFTG Microwave Measurement Symposium Digest, 2008.

[18] U. Arz and K. Kuhlmann, "Uncertainties in coplanar waveguide and microstrip line standards for on-wafer thru-reflect-line calibrations," 75th ARFTG Microwave Measurement Symposium Digest, 2010.